Diffusion-weighted imaging and the kinetic properties of MRI breast in the identification of breast cancer molecular subtypes

Safaa Mohammed Temerik*[a], Saeda Mohamed Abd Elwahab[b], Mohammed Mostafa Wahman[a], Mohammed Youssef Ahmed[c], Mostafa Elsayed Abd Elwanis[d]

[a]Clinical Oncology Department, Faculty of Medicine, South Valley University, Qena, Egypt.
[b]Diagnostic Radiology Department, Faculty of Medicine, South Valley University, Qena, Egypt.
[c]General Surgery Department, Faculty of Medicine, South Valley University, Qena, Egypt.
[d]South Egypt Cancer Institute, Faculty of Medicine, Assuit University, Assuit, Egypt

Abstract

Background: There are various molecular subtypes of breast cancer. Planning for treatment and predicting the prognosis of breast cancer all depend heavily on breast magnetic resonance imaging (MRI).

Objectives: Our study aims to establish the relevance of MRI in the initial diagnosis of breast cancer and the prognosis of the disease by examining the relationship between kinetic breast MRI features and molecular subtypes of breast cancer. The apparent diffusion coefficient (ADC) was another goal of our investigation, and we also intended to associate it with molecular subtypes.

Patients and methods: Our investigation was cross-sectional, observational, and involved only one group assignment. This study comprised 30 female patients with newly discovered invasive breast cancer. Before starting treatment, our patients underwent MRI breast. Dynamic-contrast enhanced (DCE) and diffusion-weighted (DWI) MRI tests were performed. The kind of curve and ADC were connected to the histological results and the molecular subtypes of breast cancer.

Results: Sixty-six and seven-tenth percent of our patients fit the Type II curve, and 73.3% of them had hormonal receptor (HR)-positive. Different molecular subtypes and curve types did not significantly differ from one another (p=0.107). The ADC value for mass and the various molecular subtypes showed a negligible difference (p>0.05). For triple-negative breast cancer (TNBC) and HR-negative breast cancer, the ADC value for mass was greater.

Conclusion: Limited connections were found between breast MRI kinetic criteria and molecular subtypes. Therefore, more research is required to determine the function of MRI in the early detection of breast cancer.

Keywords: Breast cancer; Molecular subtype; MRI; ADC.
DOI: 10.21608/SVUIJM.2023.222264.1620
***Correspondence**Safaatemerik@med.svu.edu.eg
Received: 14 July,2023.
Revised: 7 August, 2023.
Accepted: 12 August, 2023
Published: 18 June, 2024
Cite this article as: Safaa Mohammed Temerik, Saeda Mohamed Abd Elwahab, Mohammed Mostafa Wahman, Mohammed Youssef Ahmed, Mostafa Elsayed Abd Elwanis.(2024). Diffusion-weighted imaging and the kinetic properties of MRI breast in the identification of breast cancer molecular subtypes. *SVU-International Journal of Medical Sciences*. Vol.7, Issue 2, pp: 105-120.

Introduction

Breast cancer is considered a major health and social problem in Egypt and all over the world. Breast cancer is the leading form of cancer among women in Egypt and the primary cause of cancer-related deaths in this population (**Rostom et al., 2022**). About 46,000 new cases are expected in 2050. In comparison to other nations, Egypt's mortality/incidence rate ratio for breast cancer increased due to delayed diagnosis (**Azim et al., 2023**).

Breast cancer now has numerous molecular subgroups, histologies, and clinical outcomes. It is no longer a single illness. Human epidermal growth factor receptor 2 (HER2), progesterone receptor (PR), estrogen receptor (ER), and proliferation marker Ki-67 serve as the basis for the current clinical classification of breast cancer. Immunohistochemistry (IHC) and fluorescence in situ hybridization (FISH) are typically used to determine those **(Algazzar et al., 2020**, **Szymiczek et al., 2021**). Invasive breast cancer can be divided into four main subgroups using modern molecular profiling: HER2+, luminal A, luminal B, and TN/basal-like **(Wang et al., 2018**).

A number of imaging techniques, including sonomammography, MRI, positron emission tomography (PET), computed tomography (CT), and single-photon emission computed tomography (SPECT), might yield important information for the early identification of breast cancer (**Jafari et al., 2018**).

Breast MRI is a delicate imaging method that aids in early detection of breast cancer and evaluates the effectiveness of treatment. Additionally, it can forecast prognosis and facilitate early treatment planning (**Öztürk et al., 2020**).

With the use of DCE-MRI features, mammary cancer lesions can be analyzed morphologically and dynamically with high sensitivity (**Hu et al., 2020**). Non-enhanced and contrast-enhanced sequences are included in the usual protocol to help visualize the characteristics of breast lesions. The early, middle, and late contrast-enhanced phases of lesion enhancement are shown by the time-signal intensity curves. There are three primary types of curves: 1) Type I (persistent) with benign lesions, 2) Type II (plateau) with suspicious lesions, 3) Type III (washout) with malignant lesions (**Milon et al., 2020**).

In DWI MRI, we do not need to use contrast agents. So it is counted as less expensive and less time-consuming than DCE MRI. It relies on the movement of water molecules within the tissues (**Partovi et al., 2020**). The high cellularity and rapid proliferation of malignant tumors cause them to exhibit more limitations than benign lesions (**Deike-Hofmann et al., 2019**).

Maps that assess diffusion in living tissues are used to determine apparent diffusion coefficient (ADC). Malignant tissues result in lower ADC values because of more constrained diffusion (**Marino et al., 2018**). Earlier detection of changes in ADC values can be achieved compared to changes in tumor size or vasculature. Because of this, DWI can serve as a better early treatment guide than DCE-MRI (**Pinker et al., 2017**). There have been numerous researches on the association between mean ADC values and breast cancer molecular subtypes, yet there is a large overlap in ADC values between molecular subtypes (**Kazama et al., 2022**).

This study aimed to analyze the correlation between kinetic aspects of breast MRI and molecular subtypes of breast cancer, in order to assess the significance of MRI in the initial diagnosis and prognosis of the disease. Additionally, we calculated ADC and correlated it with molecular subtypes in this study.

Patients and methods

Patient's population: With the help of the Clinical Oncology, Radiodiagnosis, and General Surgery departments at Qena University Hospital, South Valley University, our study took place between February 2021 and February 2023. The study involved the inclusion of 30 female patients who had recently been diagnosed with invasive breast cancer. They were between the ages of twenty-two and sixty-five. True cut biopsy was used to make the diagnosis. Stage I through III was assigned to each patient's diagnosis. The study had one group assignment and was cross-sectional and observational**.**

MRI protocol

A high field system with a 1.5-T MR system (Achieva; Philips medical systems, Best, The Netherlands) was used for all breast MRI exams. For the examination, each patient was positioned prone while being examined with a special 4-channel breast surface coil. The sequences utilized include:

1) T1-weighted precontrast three-dimensional interpolated breath-hold imaging. T1-weighted gradient-echo MRI (5.5/2.7; 100° flip angle; 360° field of view; 480*480 matrix; 2° section thickness; 1° section gap).

2) T2-weighted imaging (4682/130; 15-echo train length; 360-mm field of view; 480 * 480 matrix; 2-mm slice thickness; 0-mm section gap).

3) DWI: single-shot echo-planar imaging (EPI) was used. Other parameters included b value = 0 and 800 second/mm2; slice thickness = 3 mm; slice spacing = 3 mm; TR = 5000 ms; TE = 87 ms; FOV = 250–350 mm; and the total acquisition time was 42 s.

4) Following an intravenous bolus dose of 0.1 mmol/kg gadolinium, DCE axial T1-weighted imaging with fat suppression was performed.

5) Fat suppression on a delayed, high-resolution, contrast-enhanced axial T1.

On the accompanying workstation, three circular areas of interest (ROIs) were selected based on the tumor's lowest ADC value on the ADC map, and the mean value was assessed.

Histopathological examination

Based on the results of IHC for ER, PR, HER2 expression, and the ki-67 index, different molecular subtypes were identified. The immunostaining of portions of the initial true-cut biopsy tissues was performed using a Ventana BenchMark GX autostainer. The Ventana ultraView DAB detecting system was utilized for this purpose. The most recent ASCO/CAP testing recommendations technique was used to perform ER, PR, and HER2 (**Allison et al., 2020; Wolff et al., 2018**).

If IHC was 3+, HER2 was thought to be positive. When IHC was 2+, FISH technique was used. Cancers that express ER and PR in 1%–100% of cells are referred to as HR positive cancers.

- Luminal A subtype: ER- and/or PR-positive, HER2-negative, and Ki-67 <20%.
- Luminal B subtype: either ER- and/or PR-positive, HER2-negative, and Ki-67 ≥ 20%) or ER- and/or PR-positive and HER2-positive.
- HER2-enriched type (HER2): ER- and PR-negative and HER2-positive.
- Triple-negative type (TN): ER, PR, and HER2-negative (Jackisch et al., 2015).

Data collection: The patient's history, physical examination, and initial breast sonomammography findings were recorded and updated in the medical records. The histopathology report of the original biopsy of the mass included information about the pathological type, tumor grade, Ki-67%, and hormonal receptor status (ER, PR, and HER2 neu).

Ethical considerations

1. Study approval: The South Valley University, faculty of medicine in Qena, Egypt, approved the study. (SVU-MED-ONM027-1-21-2-138 is the ethical approval code).
2. Patient Consent: Written consent was obtained from all participants in the current study after providing them with detailed information about the purpose and specifics of the investigation.

Statistical analysis

The data was collected, coded, reviewed, and entered into IBM SPSS version 26 of the Statistical Package for Social Science. For categorical variables, the data were presented as numbers and percentages; for numerical variables with parametric distribution, they were presented as mean, standard deviation, and range.

Results

The study included a cohort of 30 female breast cancer patients, whose ages ranged from twenty-two to sixty-five, with a mean age of 42.97±11.009. Nine (30%) were postmenopausal, while twenty-one (70%) were premenopausal (**Table.1**).

Table 1. Patients' demographic characteristics (N=30)

Parameters		**Number**	**Percent %**
Age (years)	**< 40**	11	36.7%
	40-50	12	40%
	>50	7	23.3 %
	Mean ± SD	42.97 ± 11.009	
	Median (range)	42.5 (22-65)	
Menopause	**Premenopausal**	21	70%
	Postmenopausal	9	30%

A type 2 curve was seen in twenty patients (66.7%), a type 3 curve in nine patients (30%), and a type 1 curve was present in just one patient (3.3%) **(Table 2, Fig.1).**

Table 2. Curve types in MRI

Parameters		**Number**	**Percent %**
Curve types	**Type 1 (benign)**	1	3.3%
	Type 2 (suspicious)	20	66.7%
	Type 3 (malignant)	9	30%

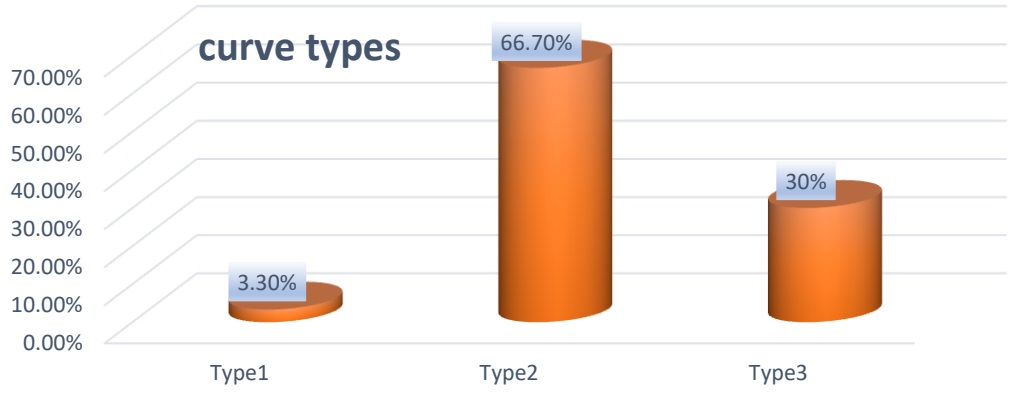

Fig. 1. Curve types in MRI

Molecular subtypes

Twenty patients (66.7%) tested positive for the estrogen receptor ER, 18 tested positive for the PR, 12 tested positive for HER2. Three patients only were diagnosed as TNBC (**Table.3).**

Table 3. Molecular subtypes among patients (N=30)

Molecular subtype		Number %	Percent %
ER status	**ER Positive**	20	66.7%
	ER negative	10	33.3%
PR status	**PR positive**	18	60%
	PR negative	12	40%
HER2 status	**HER2 positive**	12	40%
	HER2 negative	18	60%
Triple negative	**Yes**	3	10%
	No	27	90%
(HR-positive, HER2-negative)		15	50%
(HR-positive, HER2 positive)		5	16.7%
HER2-enriched		12	40%
Ki-67 index status	**<20**	18	60 %
	≥ 20	12	40%

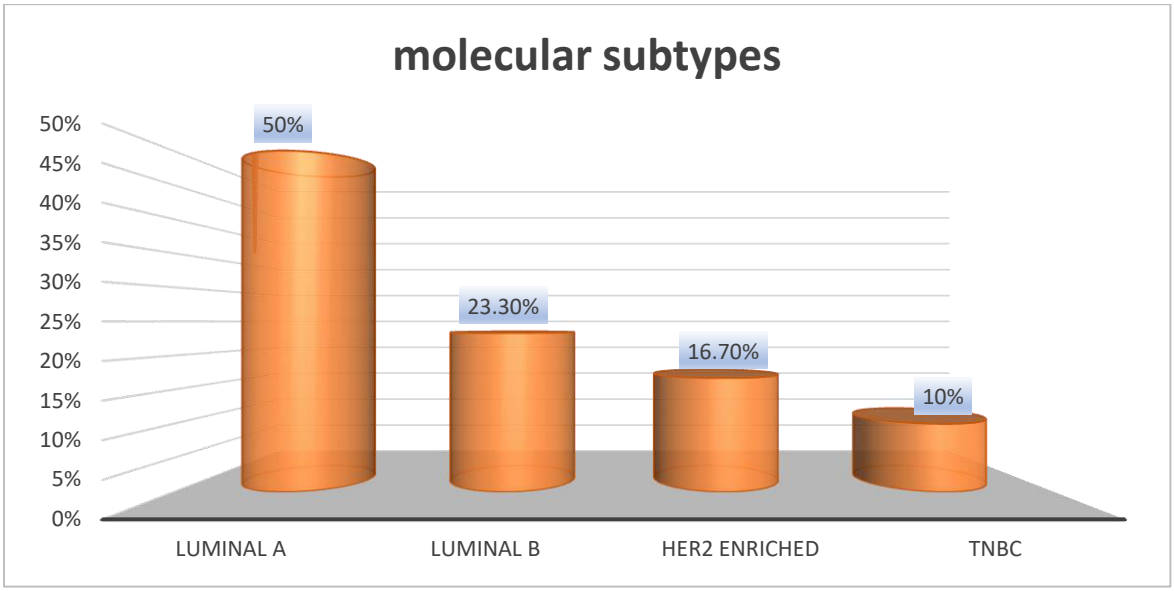

Fig.2. Molecular subtypes of breast cancer

30 breast tumors had 30 different tumor subtypes, with 15 (or 50%) having luminal A, 7 (23.3%) having luminal B, 5 (16.7%) having HER2 enrichment, and 3 (10%) having TNBC (**Fig. 2**).

Table 4. MRI kinetic and diffusion features stratified by molecular subtypes.

Morphological features		Molecular subtypes				p value
		Luminal A (n=15)	Luminal B (n=7)	HER2 enriched(n=5)	TNBC (n=3)	
		N (%)	N (%)	N (%)	N (%)	
Curve type	Type 1	0 (0%)	0 (0%)	0 (0%)	1 (33.3%)	0.107
	Type 2	11(73.3%)	4 (57.1%)	4 (80%)	1 (33.3%)	
	Type 3	4 (26.7%)	3 (42.9%)	1 (20%)	1 (33.3%)	
ADC value mass (*10^{-3} mm^2/s)	Mean ± SD	0.7767± 0.22109	0.8714 ± 0.16036	0.70 ± 0.18708	0.9333 ± 0.32146	0.377(1)
ADC value LN (*10^{-3} mm^2/s)	Mean ± SD	0.727 ± 0.1870	0.757 ± 0.1272	0.880 ± 0.3564	0.567 ± 0.4933	0.385(1)

*chi-square test- (1)one way ANOVA

Different molecular subtypes and curve types did not significantly differ from one another (p = 0.107). Compared to 57.1% of HER2-positive, 80% of HR-HER2-positive, and 33.3% of TNBC, 73.3% of HR-positive breast tumors were type 2 (**Table.4**).

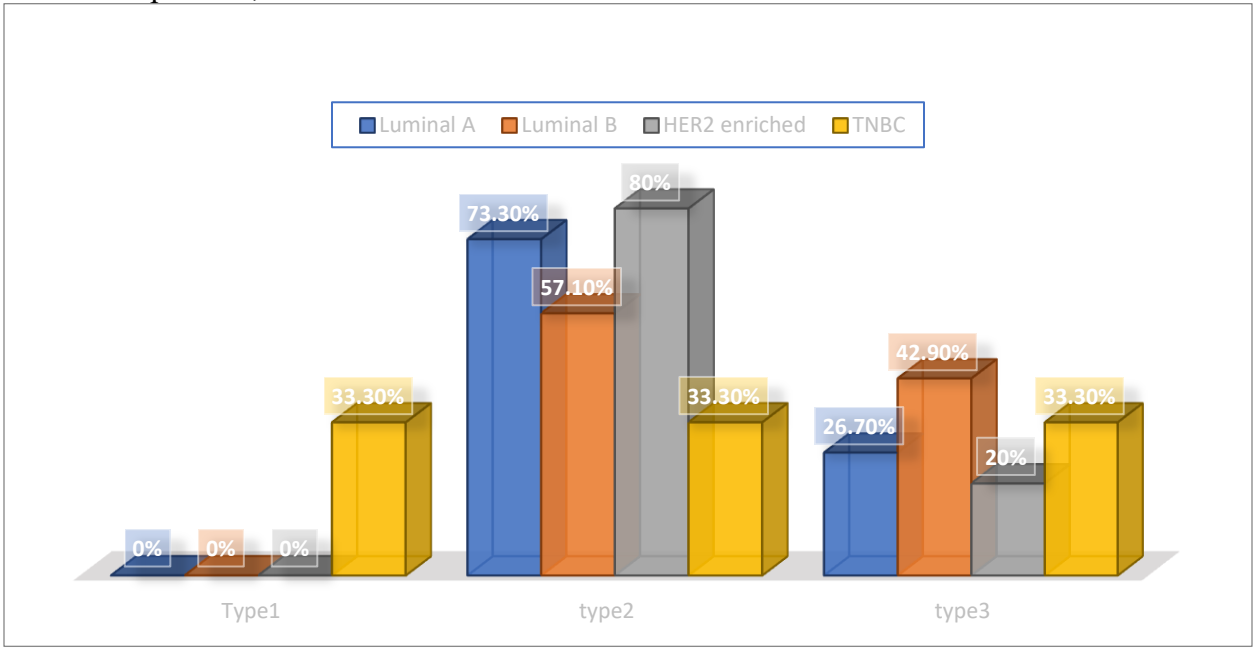

Fig.3. Curve types among different molecular subtypes

In contrast to 42.9% of HER2-positive cancers, 20% of HR-HER2-positive Regarding the ADC value for both the mass and the lymph nodes, there was a negligible difference between the molecular subtypes (p values =0.377 and 0.385, respectively). Compared to HR-positive and HER-2 tumors, and 33.3% of TNBC, 26.7% of HR-positive tumors were type 3 tumors (**Fig.3**). positive tumors, TNBC had the highest ADC value for mass (0.933±0.32146 vs. 0.7766± 0.220109, and 0.800±0.18586, respectively) as cases presented in (**Fig.s 4, 5, 6).**

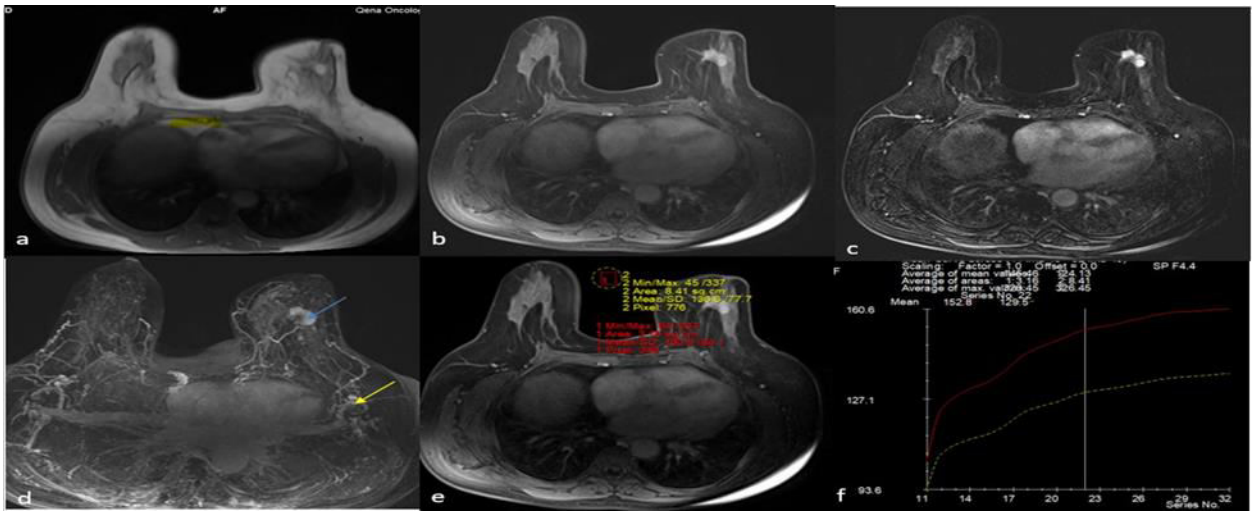

Fig. 4. A 58 – year – old female patient, presented clinically with left breast cancer. Pathologic analysis revealed infiltrating duct carcinoma (IDC), grade 2, ER+, PR+, HER 2 neu -, and Ki-67 = 20%. MRI revealed a: T1-weighted image shows an ill-defined hypointense soft mass lesion in the lower outer quadrant with irregular shape and lobulated border; b:post-contrast T1-weighted image shows homogenous intense enhancement, c: STIR image(Short Tau Inversion Recovery) shows hyperintense signal intensity, d: MIP(maximum intensity projection) post-contrast image shows hypervascular lesion; e: ADC map shows mean ADC value for the mass = 0.95 mm^2/s and mean ADC value for lymph node = 0.7 mm^2/s; f: type II curve with plateau pattern.

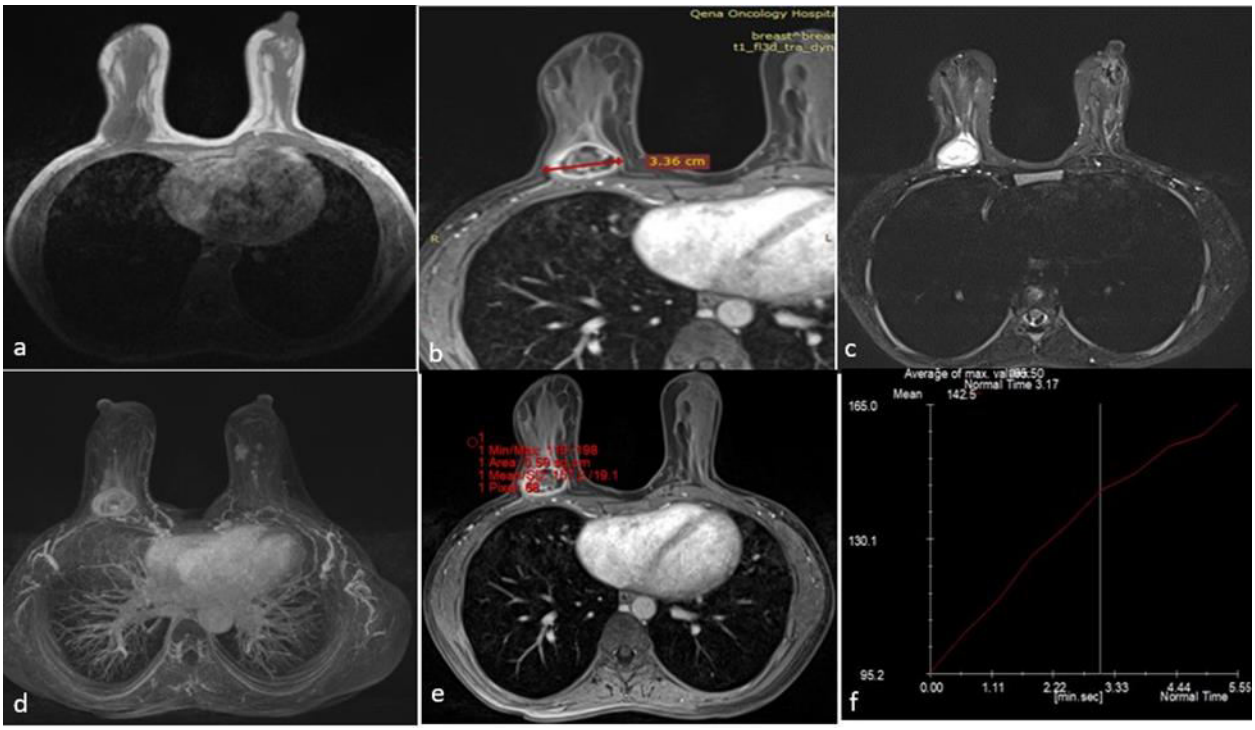

Fig.5.A 26-year-old female patient, presented clinically with right breast cancer. Pathological analysis revealed: IDC, grade 2, TN subtype, and Ki67% = 40%. MRI revealed a: T1-weighted image well-defined hypointense soft mass lesion in the lower outer quadrant with

round shape, well-defined border, and infiltrating chest wall; b:post-contrast T1-weighted image shows peripheral enhancement; c: STIR image shows hyperintense signal intensity, d: MIP post-contrast image shows increase vascularity of the lesion, e: ADC map shows mean ADC value of the lesion about 1.3 mm^2/ s; f: type I curve with persistent enhancement pattern

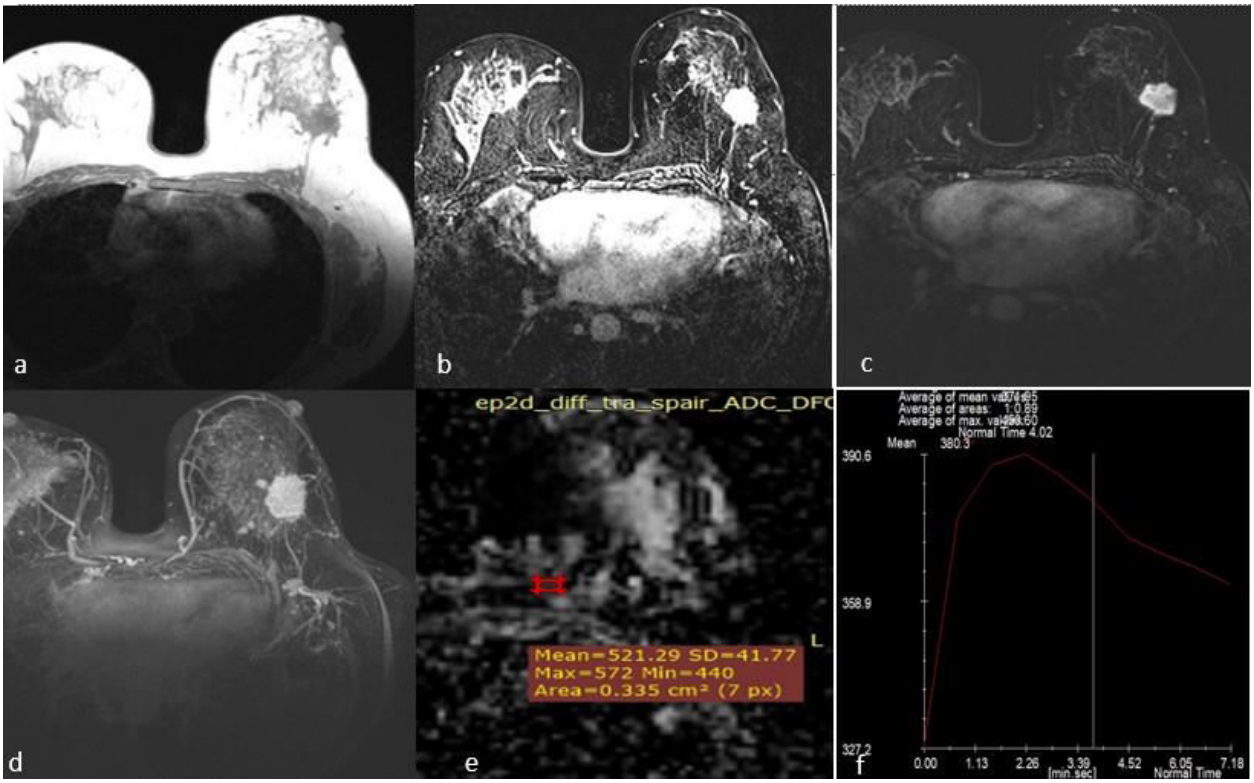

Fig.6. A 48-year-old female patient presented clinically with left breast cancer. Pathological analysis revealed: ILC, G2, ER+, PR+, Her-2-neu -, Ki67 = 15%. MRI revealed a: T1- weighted image well circumscribed hypointense solid lesion in the upper outer quadrant with a round shape and spiculated border; b: post-contrast T1-weighted image shows strong homogenous enhancement with central breaking down; c: STIR image shows hyperintense signal intensity; d: MIP post-contrast image shows increased vascularity of the lesion; e: ADC map shows mean ADC value of the mass = 0.9 mm^2/s, and mean ADC value for lymph node = 0.9 mm^2/s; f: type III curve with washout pattern.

In comparison to TNBC and HR-positive cancers, the ADC value for lymph nodes was greater with HER-2-positive tumors (**Figs. 7, 8**).

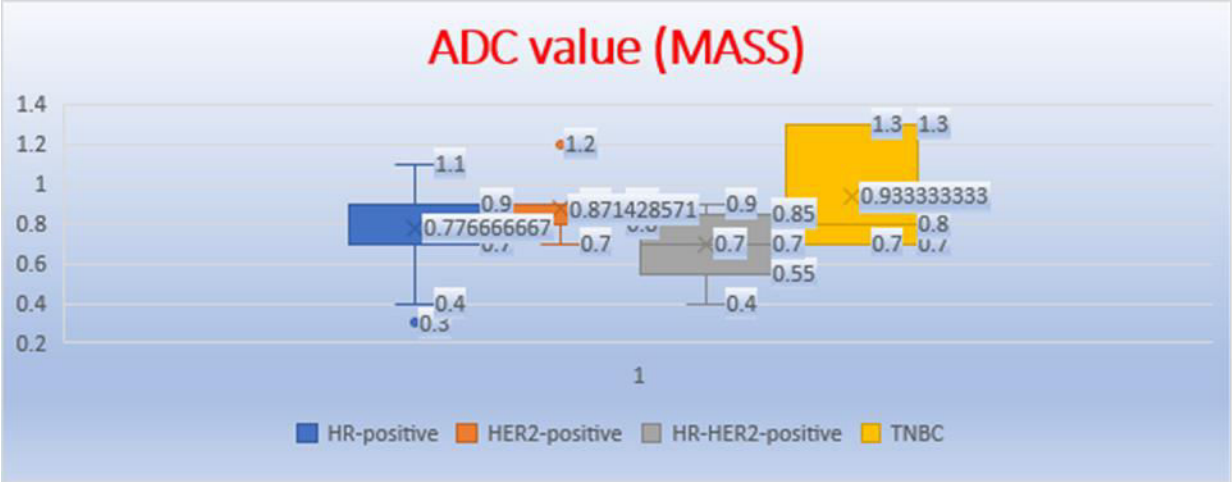

Fig.7. Box plot illustrating how several molecular subtypes differ in terms of the mass ADC value

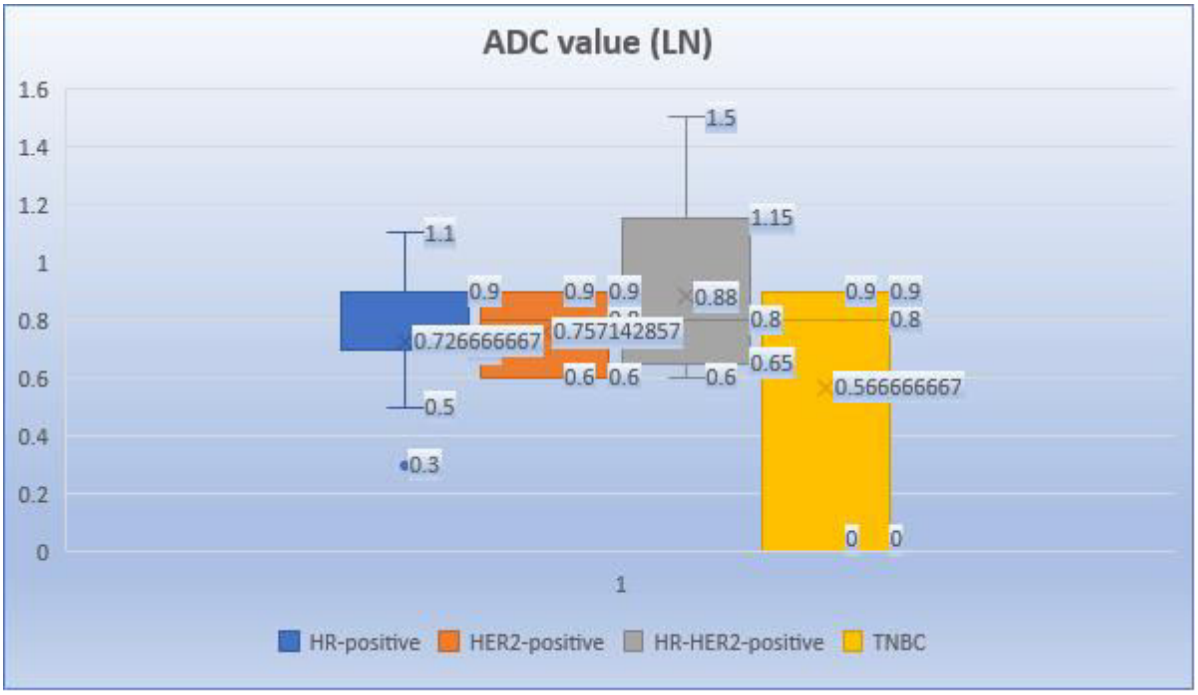

Fig.8.Box plot comparing the ADC value for lymph nodes in relation to several molecular subtypes.

The ADC value for mass and the various molecular subtypes showed a negligible difference ($p > 0.05$). With a negligible difference ($p = 0.392$), patients with ER-negative tumors had an ADC value for mass that was greater ($0.85*10^{-3}\pm 0.25495*10^{-3}$) than patients with ER-positive tumors ($0.7775*10^{-3} \pm 0.1936*10^{-3}$). Those with PR-negative tumors had an ADC value for mass that was greater ($0.8583*10^{-3}\pm 0.20652*10^{-3}$) than those with PR-positive tumors ($0.7639*10^{-3}\pm 0.2168*10^{-3}$), but the observed difference was found to be statistically insignificant ($p = 0.244$). Patients with HER2- positivity and those with HER2- negativity had similar ADC values for mass ($0.800*10^{-3} \pm 0.18586*10^{-3}$

vs. $8028*10^{-3}$ $\pm 0.23669*10^{-3}$, respectively). Patients with TNBC had somewhat greater ADC value masses than patients without TNBC ($0.9333*10^{-3}$ $\pm 32146*10^{-3}$ vs. $0.7870*10^{-3}$ $\pm 0.20267*10^{-3}$, p = 0.269) (**Table 5**).

Table 5.ADC value and breast cancer molecular subtypes are related

Parameters	**Mean ± SD**	**Mean ± SD**	**p value**
	ER status		
	ER positive (n=20)	**ER negative (n=10)**	
ADC value mass ($*10^{-3}$ mm^2/s)	0.7775± 0.1936	0.85 ± 0.25495	0.392
ADC value LN ($*10^{-3}$ mm^2/s)	0.765 ± 0.239	0.700 ± 0.2708	0.507
	PR status		
	PR positive	**PR negative**	
ADC value mass ($*10^{-3}$ mm^2/s)	0.7639 ± 0.2168	0.8583 ± 0.20652	0.244
ADC value LN ($*10^{-3}$ mm^2/s)	0.783 ± 0.2282	0.683 ± 0.2725	0.286
	HER2 status		
	HER2 positive	**HER2 negative**	
ADC value mass ($*10^{-3}$ mm^2/s)	0.800 ± 0.18586	0.8028 ± 0.23669	0.973
ADC value LN ($*10^{-3}$ mm^2/s)	0.808 ± 0.2429	0.70 ± 0.2473	0.247
	Triple negative		
	Yes	**No**	
ADC value mass ($*10^{-3}$ mm^2/s)	0.9333 ± 32146	0.7870 ± 0.20267	0.269
ADC value LN ($*10^{-3}$ mm^2/s)	0.567 ±0.4933	0.763 ± 0.2133	0.563
	Ki-67 index status		
	<20	≥20	
ADC value mass ($*10^{-3}$ mm^2/s)	0.7708 ± 0.205	0.8222 ± 0.22375	0.530
ADC value LN ($*10^{-3}$ mm^2/s)	0.750 ±0.1168	0.739 ± 0.3090	0.907

* Student t test

Histopathology

IDC (27 cases, 90%) and ILC (3 cases, 10%) were the histological classifications of the cancers. Three and three-tenths percent (1/30) of the tumors had a well-differentiated nuclear grade, while 96.7% (29/31) had a moderately-differentiated nuclear grade (**Table. 6**).

Table 6. Histopathologic factors in breast cancer (N=30)

Parameters		**Number**	**Percent %**
Histology	**IDC**	27	90%
	ILC	3	10%
Nuclear grade	**Grade 1**	1	3.3%
	Grade 2	29	96.7%
Pathological T*	**T1**	7	23.3 %
	T2	11	36.7 %
	T3	6	20%
	T4	1	3.3 %

* T4: A tumor of any size that extends directly to the chest wall and/or the skin (with ulceration or macroscopic nodules) qualifies as T4. However, invasion of the dermis alone does not meet the criteria for T4 classification (**Hortobagyi et al., 2017**). T1: Tumor 20 mm in greatest dimension, T2: Tumor >20 mm but 50 mm in greatest dimension, T3: Tumor >50 mm in greatest dimension.

Table 7 showed that the ADC value for mass and the histology of breast cancer did not significantly differ (P = 0.155). Those with IDC had a larger ADC value mass than those with ILC ($0.8204*10^{-3}$ $\pm0.20674*10^{-3}$ vs. $0.6333*10^{-3}$ $\pm0.25166*10^{-3}$). Additionally, there was no statistically significant difference between the ADC value for breast cancer mass and nuclear grade (P = 0.244). Grades 1 and 2 have different ADC value masses ($0.800*10^{-3}\pm0.00$ and $0.741*10^{-3}\pm0.2514810$-3, respectively). With regard to the lymph nodes, the ADC value for mass was insignificant (P = 0.744). Patients with positive lymph nodes exhibited a higher rate of it compared to patients with negative nodes ($0.8167*10^{-3}\pm0.17078*10^{-3}$ vs. $0.7929*10^{-3}\pm0.26447*10^{-3}$).

Table 7. Association of ADC (Apparent diffusion coefficient) value mass and ADC value lymph nodes with histopathologic prognostic factors in breast cancer

Parameters	**Mean ± SD**		**Mean ± SD**		**p value**
	Histology				
	IDC (n=27)		ILC (n=3)		
ADC value mass ($*10^{-3}mm^2/s$)	0.8204± 0.20674		0.6333 ± 0.2516		0.155(1)
ADC value LN ($*10^{-3}mm^2/s$)	0.733 ± 0.2572		0.833 ± 0.1155		0.516(1)
	Nuclear grade				
	Grade 1		Grade 2		
ADC value mass ($*10^{-3}$ mm^2/s)	0.800 ± 0.00		0.741 ± 0.2514		0.244(1)
ADC value LN ($*10^{-3}$ mm^2/s)	0.700 ± 0.00		0.8052 ± 0.21727		0.820(1)
	Lymph nodes				
	Positive		Negative		
ADC value mass ($*10^{-3}$ mm^2/s)	0.8167 ± 0.17078		0.7929 ± 0.2645		0.774(1)
ADC value LN ($*10^{-3}$ mm^2/s)	0.760 ± 0.1183		0.721 ± 0.3468		0.688(1)
	Tumor size				
	T1	T2	T3	T4	
ADC value mass ($*10^{-3}$ mm^2/s)	0.76±0.19	0.81±0.3	0.8±0.1	0.80	0.975(2)
ADC value LN ($*10^{-3}$ mm^2/s)	0.73±0.17	0.73±0.3	0.7±0.2	0.90	0.945(2)

(1) Student t test- (2) one way ANOVA

The ADC value for lymph nodes or bulk did not significantly correlate with the Ki-67 index (p = 0.986) (**Table.8**).

Table 8. A correlation exists between the Ki-67 index and the ADC value.

Parameters	**Ki-67**	
	r*	p value
ADC value for mass	-0.003	0.986
ADC value for lymph nodes	-0.048	0.801

r*Spearman correlation coefficient

Discussion

Due to the discovery of contemporary non-invasive diagnostic methods and the existence of numerous molecular subtypes of breast cancer, research in breast cancer diagnosis is rapidly developing. Finding a trustworthy link between breast MRI kinetic characteristics and molecular subtypes of breast cancer is of great interest. Our study aimed to assess the relationship between the kinetic characteristics of breast cancer observed on MRI and molecular subtypes, with the goal of predicting how this association would influence treatment decisions.

The initial enhancement phase occurs within the first two minutes following contrast injection and is categorized as slow, medium, or rapid in kinetic curves. The second component, which is referred to as persistent, plateau, or washout, depicts the delayed phase (**Erguvan-Dogan et al., 2006**). We discovered that there was no statistically significant difference between various molecular subtypes and curve types in our investigation ($p = 0.107$). In comparison to 42.9% of HER2-positive cancers, 20% of HR-HER2-positive tumors, and 33.3% of TNBC, 26.7% of HR-positive tumors were type 3 tumors.

Our results concur with those of **Navarro et al.** who found no statistically significant differences between the various MRI subtypes of the dynamic curve type ($p = 0.607$) (**Navarro Vilar et al., 2017**). Additionally, this was consistent with **Galati et al.'s** findings (**Galati et al., 2022**). According to **Algazzar et al.,** type III kinetic curves were strongly linked with HR-negative breast tumors ($p \leq 0.001$). However, the kinetic curves for HER2/neu-negative breast tumors did not show any statistical significance ($p = 0.66$) (**Algazzar et al., 2020**).

In this study, the mean ADC value was computed for both the mass and the lymph nodes, and the results were then associated with the molecular subtypes and the Ki-67 index. We discovered that, with a negligible difference ($p = 0.392$, 0.244, respectively), the mean ADC value for mass was greater for ER-negative tumors and PR-negative tumors than ER-positive and PR-positive tumors, respectively.

Additionally, we discovered that individuals with TNBC had insignificantly higher ADC values for mass compared to patients without TNBC ($p = 0.269$). Despite this, patients with HER2- positive tumors and those with HER2- negative tumors had identical ADC values. Additionally, there was a negligible correlation between the ADC value and the Ki-67 index. According to our research, **Kitajima et al.'s** study (**Kitajima et al., 2016**) found no connection between ADC and hormone expression status. **Meyer et al.'s** comprehensive study found no changes in ADC values between the tested BC types (**Meyer et al., 2022**). **Yuan et al. (Yuan et al., 2019**) discovered that there was no statistically significant link between the ADC value and molecular subtypes and immunohistochemistry variables such as ER, PR, HER2, and Ki-67. Our findings differed from those of **Du et al.** (**Du et al., 2021**) who claimed that mean ADC values were independently related to the differentiation of several molecular subtypes with a close significant difference ($p = 0.063$) between HER2-positive and HER2-negative subgroups, and that it was also related to Ki-67 expression.

This study reveals the correlation between the average ADC value and other histological results, including histology, nuclear grade, lymph node metastases, and tumor size. In our investigation, there was no discernible relationship between the mean ADC value and these results. Patients with IDC had larger ADC value masses than

patients with ILC (p = 0.155). Our findings conflict with some earlier studies, although they are consistent with others.

According to **Shin et al.,** there is a strong association between the mean ADC and histopathologically important variables such as tumor size, histological grade, and whether or not axillary lymph node metastases have occurred. They confirmed a negligible connection (p = 0.647) between the mean ADC value and histological type (**Shin and Kim, 2017**). Lower mean ADC values were found in the study by **Boria et al.** to be associated with smaller tumors (T1) (p = 0.028) and low/intermediate grade tumors (p = 0.045) (**Boria et al., 2018**). According to **Lee et al.'s** study, there is a weak correlation between the mean ADC value and lymph node metastasis (p = 0.027), but a strong correlation between the mean ADC value and tumor size and histologic grade (p = 0.196 and 0.236, respectively) (**Lee et al., 2016**). According to our research, patients with positive lymph nodes showed a slightly higher mean ADC value compared to those with negative lymph nodes, although this difference was not statistically significant (p = 0.774). In their histogram study, **Kim et al.** discovered that patients with lymph node metastases had higher ADC values for breast cancers (p = 0.058). According to **Kim et al. (2015)**, the heterogeneity of breast cancer, diverse analysis approaches, MRI methodologies, and varied approaches to determining mean ADC values are to blame for the discrepancy between the findings of various research.

This research has several restrictions. There are only a few patients in this unicenter trial. Several individuals were not included in the study because they had an excisional biopsy prior to the MRI. Some patients were excluded initially from our research because they are diagnosed as carcinoma in situ. Our continuing department has a hefty MRI examination fee. The distribution of molecular subtypes was imbalanced due to the small patient population.

Regarding the number of patients, our study included 30 patients between February 2021 and February 2023. Compared to other studies that addressed the same points in our research, it was considered a relatively small number. Some studies included a larger number of patients but over a longer period of time. For example, **Algazzar et al.** study included 60 patients from January 2017 to December 2018. The study by **Yuan et al**. involved 196 cases from August 2013 to January 2018. Fifty-two patients were incorporated in the study of **Lee et al**. between February 2012 and March 2013.

Conclusion

Particularly in the era of individualized therapy, breast MRI is playing a significant role in the field of breast cancer research. Further investigation is required to confirm the function of quantitative MRI parameters in the prediction of breast cancer initial diagnosis and prognosis, despite the study's insignificant correlations.

References

- **Algazzar MA, Elsayed EE , Alhanafy AM, Mousa WA(2020).** Breast cancer imaging features as a predictor of the hormonal receptor status, HER2neu expression, and molecular subtype. Egyptian Journal of Radiology and Nuclear Medicine, 51(1): 93.
- **Allison KH, Hammond MEH, Dowsett M, McKernin SE, Carey LA, Fitzgibbons PL, Hayes DF, et al (2020).** Estrogen and Progesterone Receptor Testing in Breast Cancer: ASCO/CAP Guideline Update. J Clin Oncol, 38 (12): 1346–1366.
- **Azim HA, Elghazawy H, Ghazy RM, Abdelaziz AH, Abdelsalam**

M, Elzorkany A, Kassem L. (2023). Clinicopathologic Features of Breast Cancer in Egypt-Contemporary Profile and Future Needs: A Systematic Review and Meta-Analysis. JCO Glob Oncol. 2023;9:e2200387.

- **Boria F, Tagliati C, Baldassarre S, Ercolani P, Marconi E, Simonetti BF, Santinelli A, et al (2018).** Morphological MR features and quantitative ADC evaluation in invasive breast cancer: Correlation with prognostic factors. Clinical Imaging, 50: 141–146.
- **Deike-Hofmann K, Koenig F, Paech D, Dreher C, Delorme S, Schlemmer HP, et al (2019)**. Abbreviated MRI Protocols in Breast Cancer Diagnostics. In Journal of Magnetic Resonance Imaging, 49 (3): 647–658.
- **Du S, Gao S, Zhang L, Yang X, Qi X, Li S (2021).** Improved discrimination of molecular subtypes in invasive breast cancer: Comparison of multiple quantitative parameters from breast MRI. Magnetic Resonance Imaging, 77: 148–158.
- **Erguvan-Dogan B, Whitman GJ, Kushwaha AC, Phelps MJ, Dempsey PJ (2006)**. BI-RADS-MRI: a primer. AJR. American Journal of Roentgenology, 187(2): 152–160.
- **Galati F, Rizzo V, Moffa G, Caramanico C, Kripa E, Cerbelli B, et al (2022).** Radiologic-pathologic correlation in breast cancer: do MRI biomarkers correlate with pathologic features and molecular subtypes? European Radiology Experimental, 6(1): 39.
- **Hortobagyi GN et al., 2017.** Breast. In AJCC Cancer Staging Manual. 8th edition. Germany, Springer International Publishing., pp. 589–636.
- **Hu Q, Whitney HM, Giger ML (2020).** A deep learning methodology for improved breast cancer diagnosis using multiparametric MRI. Scientific Reports, 10(1): 10536.
- **Jackisch C, Harbeck N, Huober J, von Minckwitz G, Gerber B, Kreipe HH, Liedtke C, et al (2015).** 14th St. Gallen International Breast Cancer Conference 2015: Evidence, Controversies, Consensus - Primary Therapy of Early Breast Cancer: Opinions Expressed by German Experts. Breast Care (Basel), 10(3): 211–219.
- **Jafari SH, Saadatpour Z, Salmaninejad A, Momeni F, Mokhtari M, Nahand JS, et al (2018).** Breast cancer diagnosis: Imaging techniques and biochemical markers. Journal of Cellular Physiology, 233(7): 5200–5213.
- **Kazama T, Takahara T, Hashimoto J (2022).** Breast Cancer Subtypes and Quantitative Magnetic Resonance Imaging: A Systemic Review. Life, 12 (4): 490.
- **Kim EJ, Kim SH, Park GE, Kang BJ, Song BJ, Kim YJ, et al (2015).** Histogram analysis of apparent diffusion coefficient at 3.0t: Correlation with prognostic factors and subtypes of invasive ductal carcinoma. Journal of Magnetic Resonance Imaging, 42(6): 1666–1678.
- **Kitajima K, Yamano T, Fukushima K, Miyoshi Y, Hirota S, Kawanaka Y, et al.(2016).** Correlation of the SUVmax of

FDG-PET and ADC values of diffusion-weighted MR imaging with pathologic prognostic factors in breast carcinoma. European Journal of Radiology, 85(5): 943–949.

- **Lee HS, Kim SH, Kang BJ, Baek JE, Song BJ (2016).** Perfusion Parameters in Dynamic Contrast-enhanced MRI and Apparent Diffusion Coefficient Value in Diffusion-weighted MRI: Association with Prognostic Factors in Breast Cancer. Academic Radiology, 23(4): 446–456.
- **Marinon MA, Helbich T, Baltzer P, Pinker-Domenig K (2018)**. Multiparametric MRI of the breast: A review. Journal of Magnetic Resonance Imaging, 47(2): 301–315.
- **Meyer HJ, Wienke A, Surov A (2022)**. Diffusion-Weighted Imaging of Different Breast Cancer Molecular Subtypes: A Systematic Review and Meta-Analysis. Breast Care,17(1): 47–54.
- **Milon A, Wahab CA, Kermarrec E, Bekhouche A, Taourel P, Thomassin-Naggara I (2020).** Breast MRI: Is faster better? American Journal of Roentgenology, 214 (2): 282–295.
- **Navarro VL, Alandete SP, Medina R, Blanc E, Camarasa N, Vilar J .(2017).** MR Imaging Findings in Molecular Subtypes of Breast Cancer According to BIRADS System. Breast Journal, 23(4), 421–428.
- **Öztürk VS, Polat YD, Soyder A, Tanyeri A, Karaman CZ, Taşkın F (2020).** The Relationship Between MRI Findings and Molecular Subtypes in Women With Breast Cancer. Current Problems in Diagnostic Radiology, 49(6): 417–421.
- **Partovi S, Sin D, Lu Z, Sieck L, Marshall H, Pham R, et al (2020).** Fast MRI breast cancer screening – Ready for prime time. Clinical Imaging, 60 (2): 160–168.
- **Pinker K, Helbich TH, Morris EA (2017).** The potential of multiparametric MRI of the breast. British Journal of Radiology, 90(1069): 20160715.
- **Rostom Y, Abdelmoneim SE, Shaker M, Mahmoud N.(2022).** Presentation and management of female breast cancer in Egypt. Eastern Mediterranean Health Journal, 28(10): 725–732.
- **Shin JK, Kim JY. (2017)**. Dynamic contrast-enhanced and diffusion-weighted MRI of estrogen receptor-positive invasive breast cancers: Associations between quantitative MR parameters and Ki-67 proliferation status. Journal of Magnetic Resonance Imaging, 45(1): 94–102.
- **Szymiczek A, Lone A, Akbari MR (2021).** Molecular intrinsic versus clinical subtyping in breast cancer: A comprehensive review. Clinical Genetics, 99 (5): 613–637.
- **Wang C, Wei W, Santiago L, Whitman G, Dogan B. (2018).** Can imaging kinetic parameters of dynamic contrast-enhanced magnetic resonance imaging be valuable in predicting clinicopathological prognostic factors of invasive breast cancer? Acta Radiologica, 59(7): 813–821.
- **Wolff AC, Hammond MEH, Allison KH, Harvey BE, Mangu PB, Bartlett JMS, et al. (2018)**. Human epidermal growth factor receptor 2 testing in breast cancer:

American Society of clinical oncology/College of american pathologists clinical practice guideline focused update. J Clin Oncol, 36: 2105–2122.

- **Yuan C, Jin F, Guo X, Zhao S, Li W, Guo H. (2019).** Correlation Analysis of Breast Cancer DWI Combined with DCE-MRI Imaging Features with Molecular Subtypes and Prognostic Factors. Journal of Medical Systems, 43(4): 83.